Multiplicity dependence of charm production in pp scattering at 7 TeV and parton saturation

K.W. in collaboration with

T. Pierog, Iu. Karpenko, B. Guiot, G. Sophys

D multiplicity vs charged multiplicity in pp

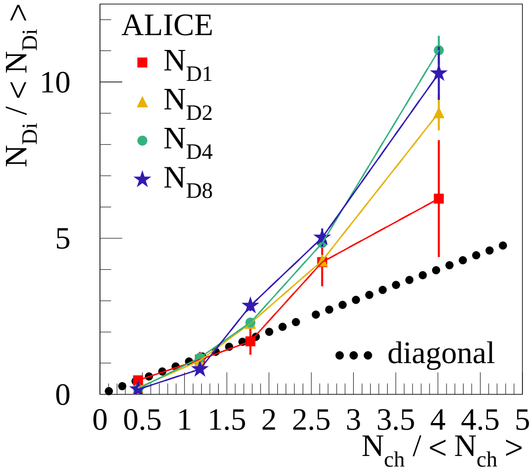

ALICE arXiv:1505.00664v1

Significant deviation from the diagonal (linear increase)

in particular for large p_t

Similar observations for J/Ψ and Υ

PYTHIA 8.157

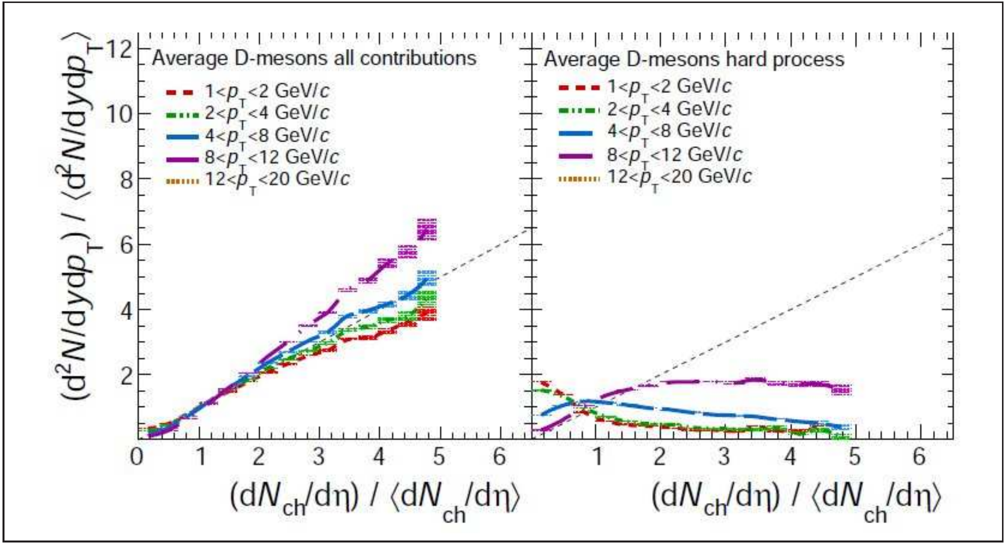
Average D-mesons all contributions
1<p_T<2 GeV/c
2<p_T<4 GeV/c
4<p_T<8 GeV/c
8<p_T<12 GeV/c
12<p_T<20 GeV/c
Average D-mesons hard process
(d²N/dydp_T) / ⟨d²N/dydp_T⟩
(dN_ch/dη) / ⟨dN_ch/dη⟩

Already understanding
a linear increase is a challenge!

(Only recent Pythia versions can do)

Even much more the
deviation from linear (towards higher values)

Trying to understand these data in the EPOS framework

Important issues:

- ☐ **Multiple scattering, parton saturation**
- ☐ **Collectivity**

Part I

EPOS Overview

EPOS: Based on multiple scattering and flow

Several steps (even in pp!):

1) Initial conditions:
Gribov-Regge **multiple scattering** approach,
elementary object = Pomeron = parton ladder,
Nonlinear effects via saturation scale Q_s

2) Core-corona approach
to separate fluid and jet hadrons

3) Viscous **hydrodynamic expansion**, $\eta/s = 0.08$

4) Statistical hadronization, final state hadronic cascade

arXiv:1312.1233 , arXix:1307.4379

Initial conditions: Marriage pQCD+GRT+energy sharing

(Drescher, Hladik, Ostapchenko, Pierog, and Werner, Phys. Rept. 350, 2001)

For pp, pA, AA:

$$\sigma^{\mathrm{tot}} = \sum_{\mathrm{cut\,P}} \int \sum_{\mathrm{uncut\,P}} \int$$

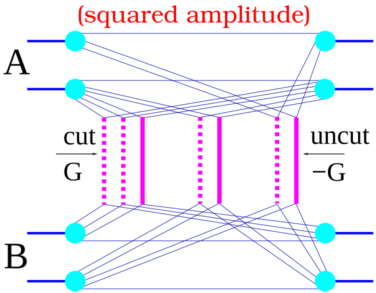

$d\sigma_{\mathrm{exclusive}}$

$$\mathrm{cut\,Pom}: G = \frac{1}{2\hat{s}} 2\mathrm{Im}\,\{\mathcal{FT}\{T\}\}(\hat{s}, b),\ T = i\hat{s}\,\sigma_{hard}(\hat{s})\ \exp(R^2_{\mathrm{hard}} t)$$

Nonlinear effects considered via saturation scale Q_s

$$
\begin{aligned}
\sigma^{\mathrm{tot}} = \int d^2b \int \prod_{i=1}^{A} d^2b_i^A\, dz_i^A\, \rho_A\big(\sqrt{(b_i^A)^2+(z_i^A)^2}\big) \\
\prod_{j=1}^{B} d^2b_j^B\, dz_j^B\, \rho_B\big(\sqrt{(b_j^B)^2+(z_j^B)^2}\big) \\
\sum_{m_1 l_1} \ldots \sum_{m_{AB} l_{AB}} (1-\delta_{0\Sigma m_k}) \int \prod_{k=1}^{AB} \left(\prod_{\mu=1}^{m_k} dx_{k,\mu}^{+} dx_{k,\mu}^{-} \prod_{\lambda=1}^{l_k} d\tilde{x}_{k,\lambda}^{+} d\tilde{x}_{k,\lambda}^{-} \right) \Bigg\{ \\
\prod_{k=1}^{AB} \left(\frac{1}{m_k!} \frac{1}{l_k!} \prod_{\mu=1}^{m_k} G(x_{k,\mu}^{+}, x_{k,\mu}^{-}, s, |\vec{b}+\vec{b}_{\pi(k)}^{A} - \vec{b}_{\tau(k)}^{B}|) \right. \\
\left. \prod_{\lambda=1}^{l_k} -G(\tilde{x}_{k,\lambda}^{+}, \tilde{x}_{k,\lambda}^{-}, s, |\vec{b}+\vec{b}_{\pi(k)}^{A} - \vec{b}_{\tau(k)}^{B}|) \right) \\
\prod_{i=1}^{A} \left(1 - \sum_{\pi(k)=i} x_{k,\mu,}^{+} - \sum_{\pi(k)=i} \tilde{x}_{k,\lambda}^{+} \right)^{\alpha} \prod_{j=1}^{B} \left(1 - \sum_{\tau(k)=j} x_{k,\mu}^{-} - \sum_{\tau(k)=j} \tilde{x}_{k,\lambda}^{-} \right)^{\alpha} \Bigg\}
\end{aligned}
$$

Core-corona procedure (for pp, pA, AA):

Pomeron => parton ladder => flux tube (kinky string)

String segments with high pt escape => **corona**, the others form the **core** = initial condition for hydro depending on the local string density

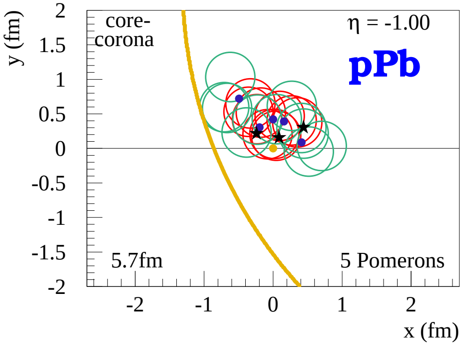

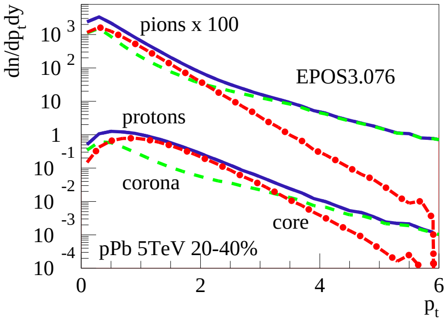

Core => Hydro evolution (Yuri Karpenko)

Israel-Stewart formulation, $\eta - \tau$ coordinates, $\eta/S = 0.08$, $\zeta/S = 0$

$$\partial_{;\nu} T^{\mu\nu} = \partial_\nu T^{\mu\nu} + \Gamma^{\mu}_{\nu\lambda} T^{\nu\lambda} + \Gamma^{\nu}_{\nu\lambda} T^{\mu\lambda} = 0$$

$$\gamma\left(\partial_t + v_i \partial_i\right) \pi^{\mu\nu} = -\frac{\pi^{\mu\nu} - \pi^{\mu\nu}_{\mathrm{NS}}}{\tau_\pi} + I^{\mu\nu}_\pi \qquad \gamma\left(\partial_t + v_i \partial_i\right) \Pi = -\frac{\Pi - \Pi_{\mathrm{NS}}}{\tau_\Pi} + I_\Pi$$

- ☐ $T^{\mu\nu} = \epsilon u^\mu u^\nu - (p + \Pi)\Delta^{\mu\nu} + \pi^{\mu\nu}$,
- ☐ $\partial_{;\nu}$ denotes a covariant derivative,
- ☐ $\Delta^{\mu\nu} = g^{\mu\nu} - u^\mu u^\nu$ is the projector orthogonal to u^μ,
- ☐ $\pi^{\mu\nu}$, Π shear stress tensor, bulk pressure
- ☐ $\pi^{\mu\nu}_{\mathrm{NS}} = \eta(\Delta^{\mu\lambda}\partial_{;\lambda}u^\nu + \Delta\nu\lambda\partial_{;\lambda}u^\mu) - \frac{2}{3}\eta\Delta^{\mu\nu}\partial_{;\lambda}u^\lambda$
- ☐ $\Pi_{\mathrm{NS}} = -\zeta\partial_{;\lambda}u^\lambda$
- ☐ $I^{\mu\nu}_\pi = -\frac{4}{3}\pi^{\mu\nu}\partial_{;\gamma}u^\gamma - [u^\nu\pi^{\mu\beta} + u^\mu\pi^{\nu\beta}]u^\lambda\partial_{;\lambda}u_\beta$
- ☐ $I_\Pi = -\frac{4}{3}\Pi\partial_{;\gamma}u^\gamma$

Freeze out: at 168 MeV, Cooper-Frye $E\frac{dn}{d^3p} = \int d\Sigma_\mu p^\mu f(up)$, equilibrium distr

Hadronic afterburner: UrQMD

Marcus Bleicher, Jan Steinheimer

Results

Detailed studies of **pt spectra**
and **azimuthal anisotropies** (dihadron corr., v_n) in pp, pA:

- ☐ arXiv:1312.1233 [nucl-th]. Published in Phys.Rev. C89 (2014) 6, 064903.
- ☐ arXiv:1307.4379 [nucl-th]. Published in Phys.Rev.Lett. 112 (2014) 23, 232301.
- ☐ arXiv:1011.0375 [hep-ph]. Published in Phys.Rev.Lett. 106 (2011) 122004
- ☐ arXiv:1004.0805 [nucl-th]. Published in Phys.Rev. C82 (2010) 044904.

In the follwing : An example of an
asymmetric space-time evolution (high mult pp event, 7TeV)

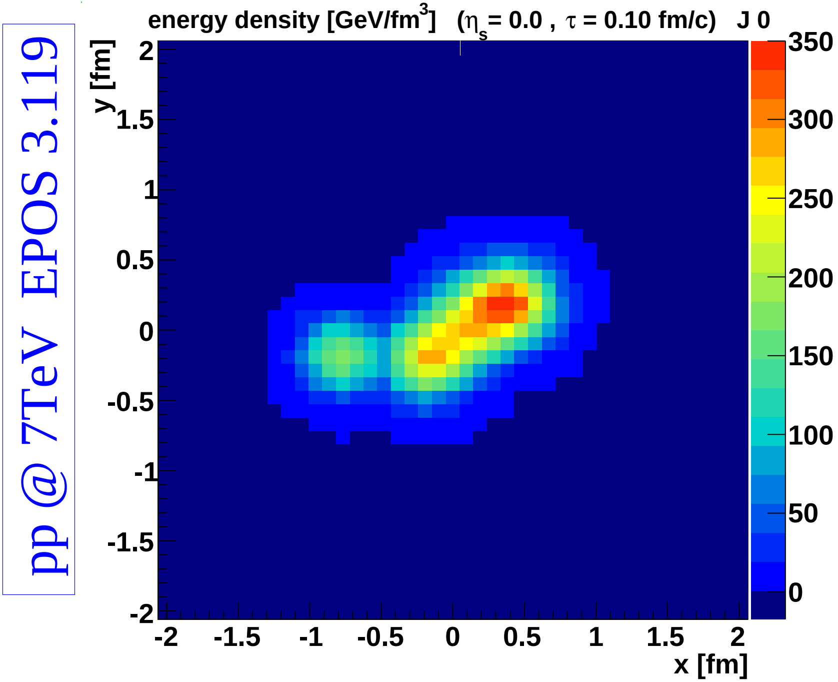

pp @ 7TeV EPOS 3.119
energy density [GeV/fm^3] (η_s = 0.0 , τ = 0.10 fm/c) J 0
y [fm]
x [fm]
2
1.5
1
0.5
0
-0.5
-1
-1.5
-2
350
300
250
200
150
100
50
0

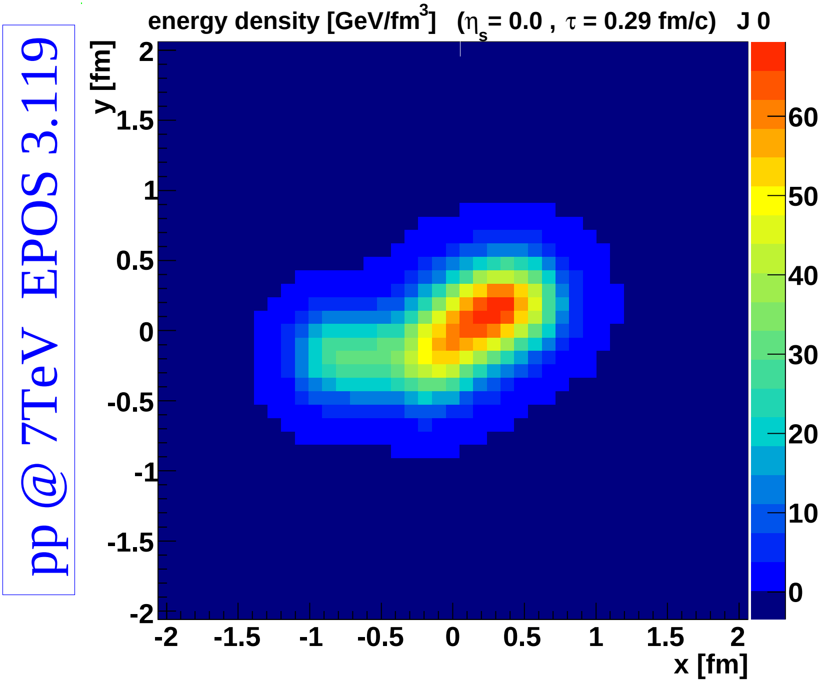

pp @ 7TeV EPOS 3.119
energy density [GeV/fm^3] (η_s = 0.0 , τ = 0.29 fm/c) J 0
y [fm]
x [fm]
2
1.5
1
0.5
0
-0.5
-1
-1.5
-2
60
50
40
30
20
10
0

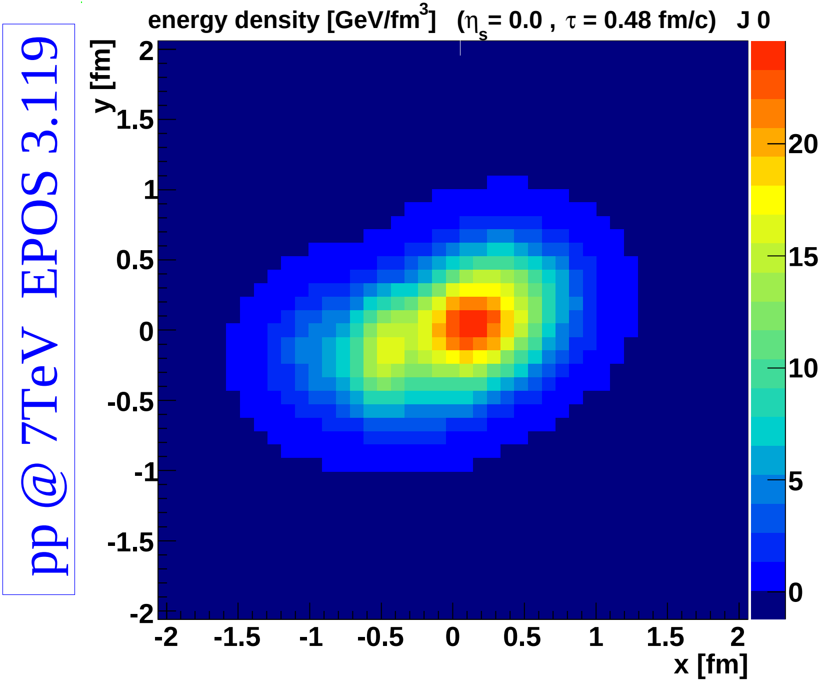
pp @ 7TeV EPOS 3.119
energy density [GeV/fm^3] (η_s = 0.0 , τ = 0.48 fm/c) J 0
y [fm]
x [fm]
2
1.5
1
0.5
0
-0.5
-1
-1.5
-2
20
15
10
5
0

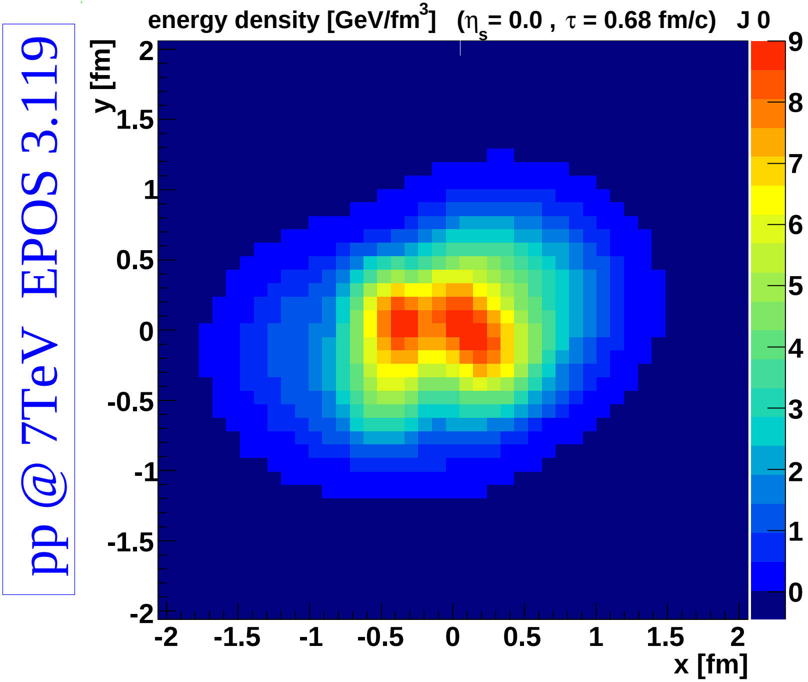
pp @ 7TeV EPOS 3.119
energy density [GeV/fm3] (ηs = 0.0 , τ = 0.68 fm/c) J 0
y [fm]
x [fm]
2
1.5
1
0.5
0
-0.5
-1
-1.5
-2
9
8
7
6
5
4
3
2
1
0

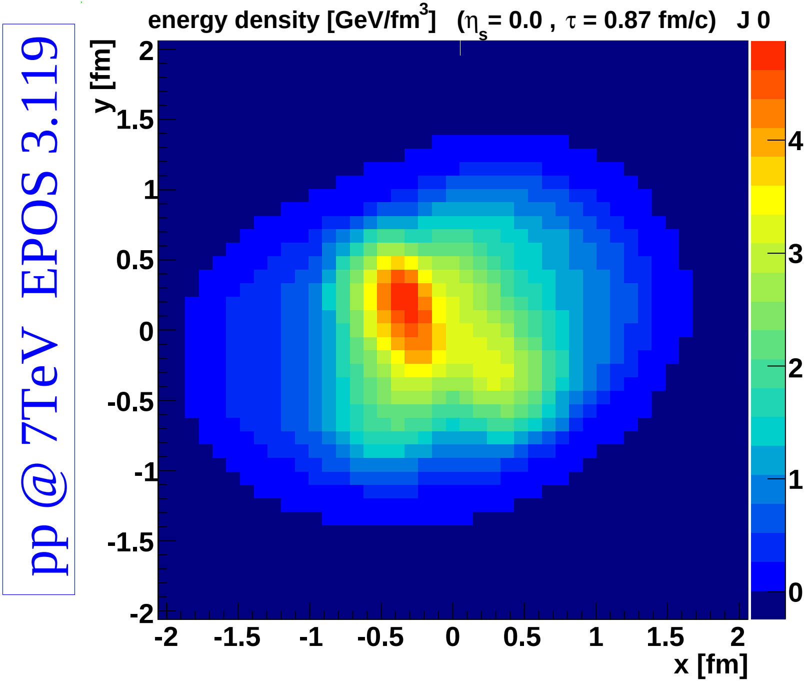
pp @ 7TeV EPOS 3.119
energy density [GeV/fm^3] (η_s = 0.0 , τ = 0.87 fm/c) J 0
y [fm]
2
1.5
1
0.5
0
-0.5
-1
-1.5
-2
-2
-1.5
-1
-0.5
0
0.5
1
1.5
2
x [fm]
4
3
2
1
0

pp @ 7TeV EPOS 3.119

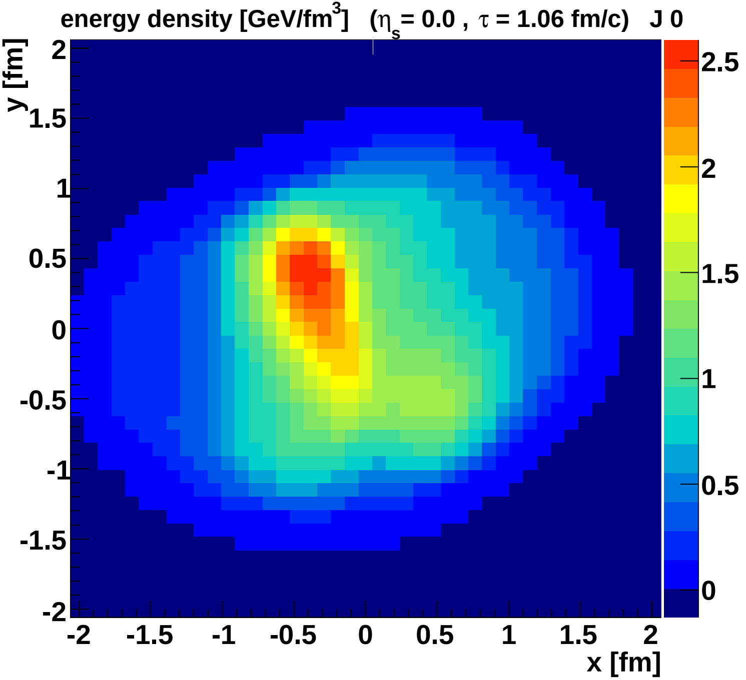

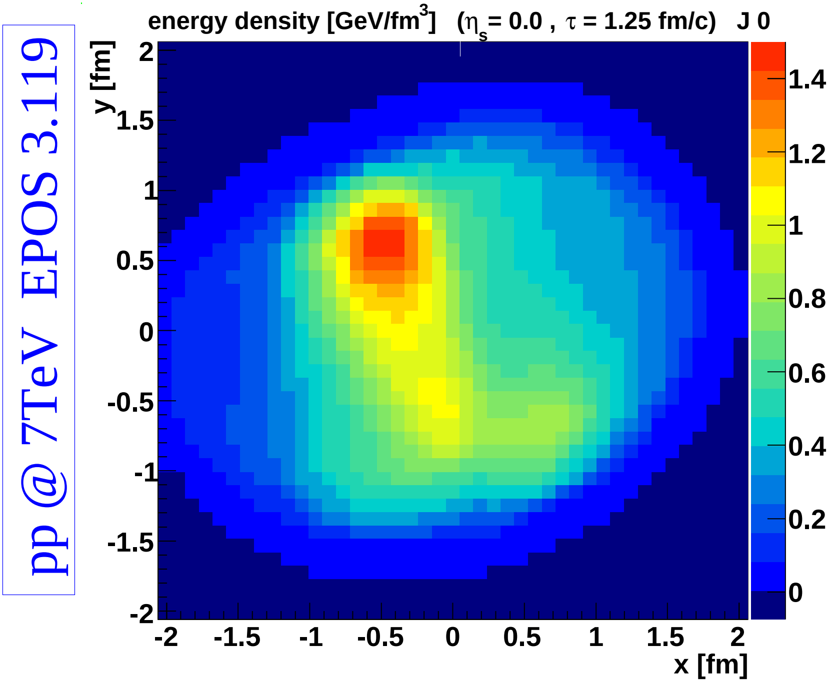
pp @ 7TeV EPOS 3.119
energy density [GeV/fm³] (ηs = 0.0 , τ = 1.25 fm/c) J 0
y [fm]
x [fm]
2
1.5
1
0.5
0
-0.5
-1
-1.5
-2
-2
-1.5
-1
-0.5
0
0.5
1
1.5
2
1.4
1.2
1
0.8
0.6
0.4
0.2
0

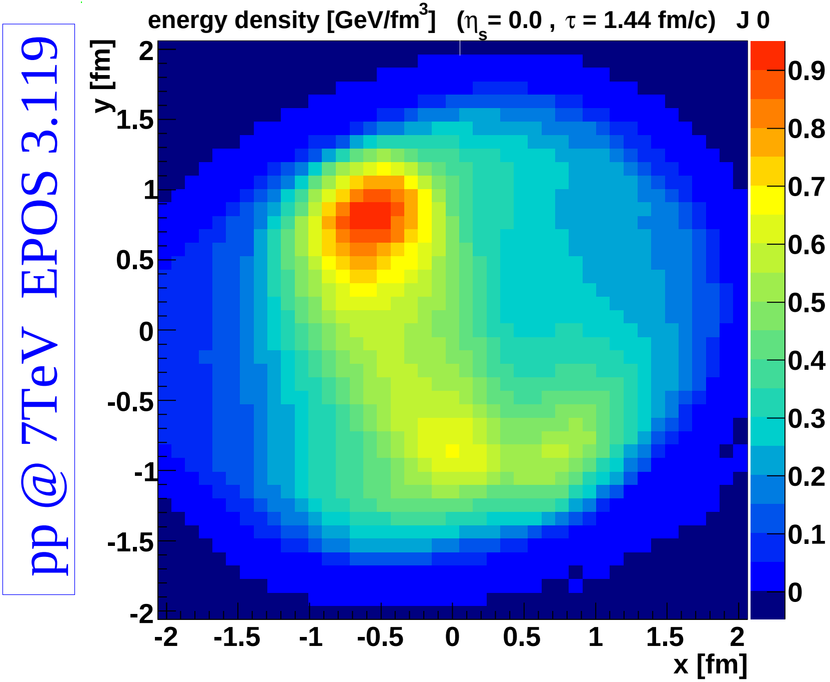
pp @ 7TeV EPOS 3.119
energy density [GeV/fm^3] (η_s = 0.0 , τ = 1.44 fm/c) J 0
y [fm]
x [fm]
2
1.5
1
0.5
0
-0.5
-1
-1.5
-2
-2 -1.5 -1 -0.5 0 0.5 1 1.5 2
0.9
0.8
0.7
0.6
0.5
0.4
0.3
0.2
0.1
0

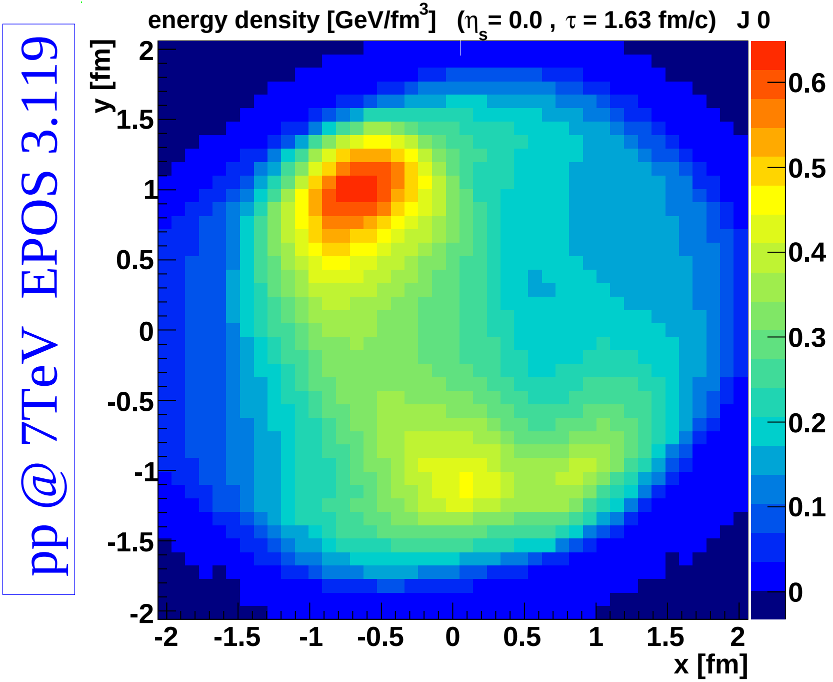
pp @ 7TeV EPOS 3.119
energy density [GeV/fm^3] (η_s = 0.0 , τ = 1.63 fm/c) J 0
y [fm]
x [fm]
2
1.5
1
0.5
0
-0.5
-1
-1.5
-2
0.6
0.5
0.4
0.3
0.2
0.1
0

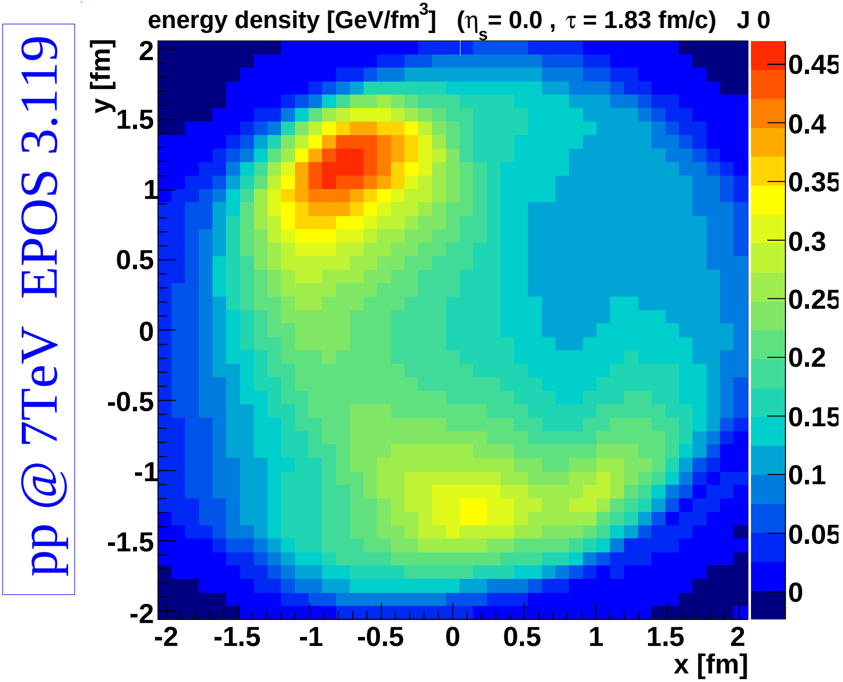
pp @ 7TeV EPOS 3.119
energy density [GeV/fm^3] (η_s = 0.0 , τ = 1.83 fm/c) J 0
y [fm]
x [fm]
2
1.5
1
0.5
0
-0.5
-1
-1.5
-2
-2
-1.5
-1
-0.5
0
0.5
1
1.5
2
0.45
0.4
0.35
0.3
0.25
0.2
0.15
0.1
0.05
0

pp @ 7TeV EPOS 3.119

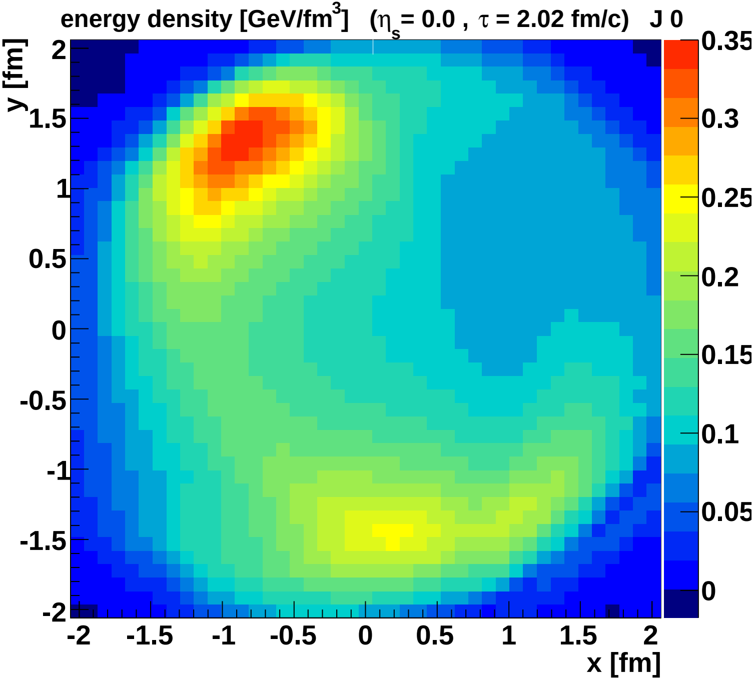

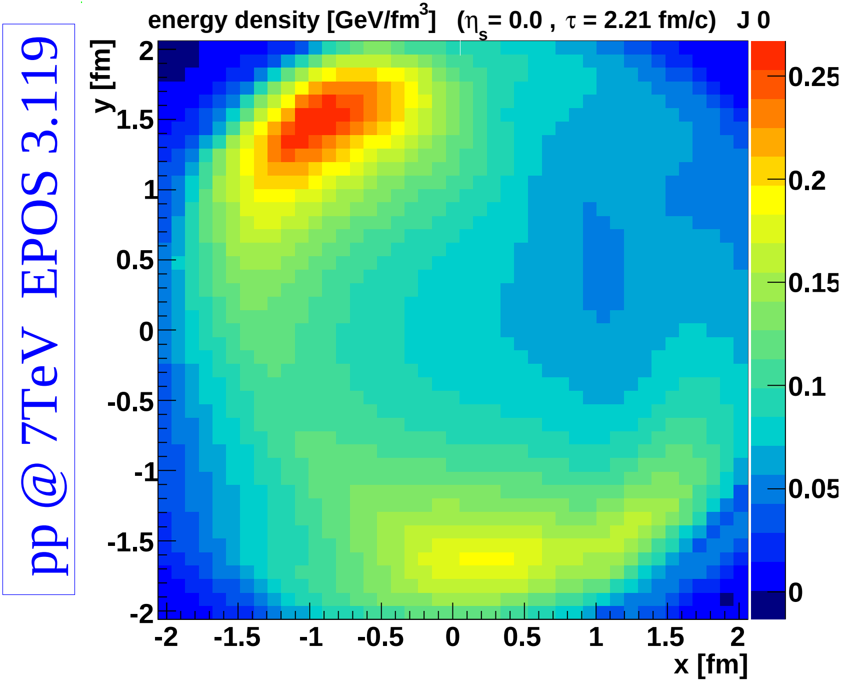
pp @ 7TeV EPOS 3.119
energy density [GeV/fm^3] (η_s = 0.0 , τ = 2.21 fm/c) J 0
y [fm]
x [fm]
2
1.5
1
0.5
0
-0.5
-1
-1.5
-2
0.25
0.2
0.15
0.1
0.05
0

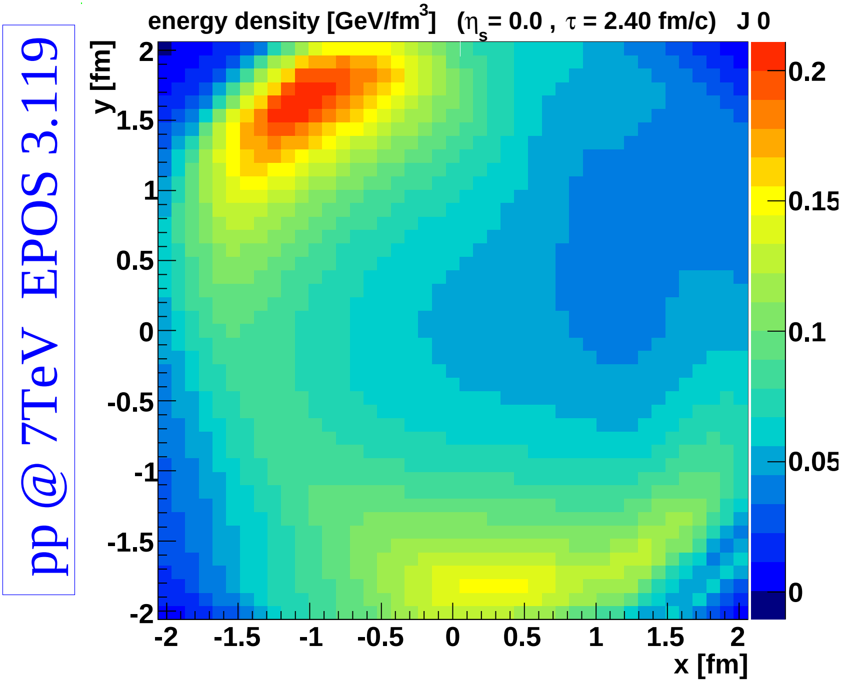

pp @ 7TeV EPOS 3.119
energy density [GeV/fm³] (ηs = 0.0 , τ = 2.40 fm/c) J 0
y [fm]
x [fm]
-2
-1.5
-1
-0.5
0
0.5
1
1.5
2
0
0.05
0.1
0.15
0.2

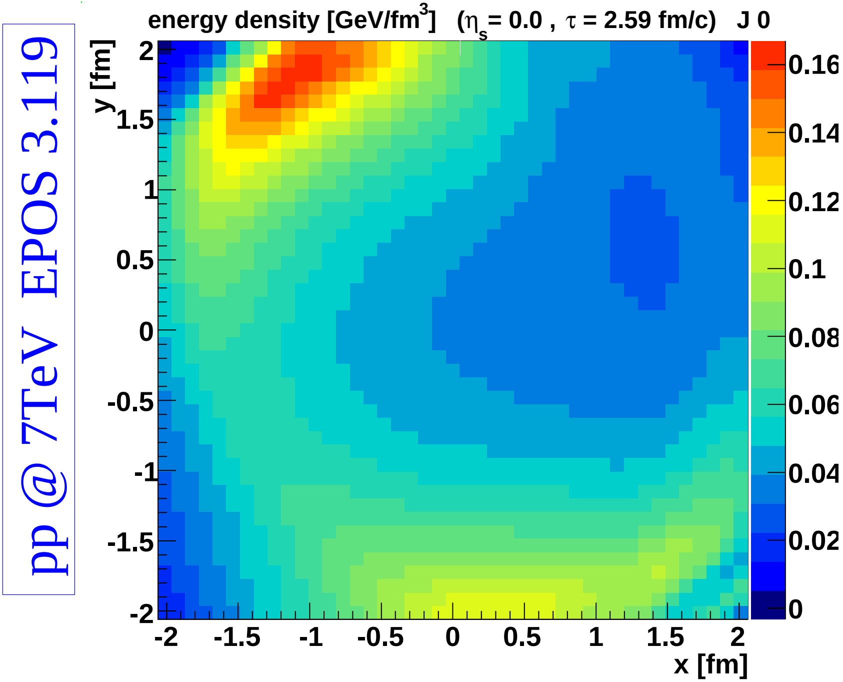
pp @ 7TeV EPOS 3.119
energy density [GeV/fm^3] (η_s = 0.0 , τ = 2.59 fm/c) J 0
y [fm]
x [fm]
2
1.5
1
0.5
0
-0.5
-1
-1.5
-2
0.16
0.14
0.12
0.1
0.08
0.06
0.04
0.02
0

Part II

A crucial ingredient: The saturation scale Q_s^2

Some facts about the Gribov-Regge multiple scattering scheme (the heart of the EPOS approach)

S-matrix:

$$|\psi(t=+\infty)\rangle = \hat{S}\,|\psi(t=-\infty)\rangle$$

Unitarity relation:

$$\hat{S}^{\dagger}\hat{S} = 1$$

which leads to ($\sum$ includes phase space integration)

$$\begin{aligned}
\underbrace{\sum_f (2\pi)^4 \delta(p_f - p_i) \, |T_{fi}|^2}_{2s\,\sigma_{\mathrm{tot}}} &= \frac{1}{i}\left(T_{ii} - T_{ii}^*\right) \\
&= 2\mathrm{Im} T_{ii} \\
&= \frac{1}{\mathrm{i}} \mathrm{disc}\, T_{ii}
\end{aligned}$$

with (s, t : Mandelstam variables)

$$\mathrm{disc}\, T_{ii} = T_{ii}(s + i\epsilon, t) - T_{ii}(s - i\epsilon, t)$$

In detail :

$$\begin{aligned} 1 &= \langle i|\,\hat{S}^{\dagger}\hat{S}\,|i\rangle \\ &= \sum_f \langle i|\,\hat{S}^{\dagger}\,|f\rangle\,\langle f|\,\hat{S}\,|i\rangle \\ &= \sum_f \langle f|\,\hat{S}\,|i\rangle^{*}\,\langle f|\,\hat{S}\,|i\rangle \end{aligned}$$

So

$$1 = \sum_f S^{*}_{fi} S_{fi}$$

Using $S_{fi} = \delta_{fi} + i(2\pi)^4\delta(p_f - p_i)T_{fi}$, dividing by $i(2\pi)^4\delta(0)$

$$\begin{aligned} \frac{1}{i}\left(T_{ii} - T^{*}_{ii}\right) &= \sum_f (2\pi)^4\delta(p_f - p_i)\,|T_{fi}|^2 \\ &= 2w\,\sigma_{\mathrm{tot}} \\ &= 2s\sigma_{\mathrm{tot}} \end{aligned}$$

The l.h.s. :

$$\frac{1}{i}\left(T_{ii} - T^{*}_{ii}\right) = 2\mathrm{Im}T_{ii}$$

So we get the optical theorem

$$2\mathrm{Im}T_{ii} = \sum_f (2\pi)^4 \delta(p_f - p_i)\,|T_{fi}|^2 = 2s\,\sigma_{\mathrm{tot}}$$

Assume:

- T_{ii} is Lorentz invariant $\rightarrow$ use s, t
- $T_{ii}(s,t)$ is an analytic function of s, with s considered as a complex variable (Hermitean analyticity)
- $T_{ii}(s,t)$ is real on some part of the real axis (see optical theorem)

Using the Schwarz reflection principle, $T_{ii}(s,t)$ first defined for $\mathrm{Im}s \geq 0$ can be continued in a unique fashion via $T_{ii}(s^*,t) = T_{ii}(s,t)^*$. So:

$$\frac{1}{i}\left(T_{ii}(s,t) - T_{ii}(s,t)^*\right) = \frac{1}{i}\left(T_{ii}(s,t) - T_{ii}(s^*,t)\right) = \frac{1}{i}\mathrm{disc}\,T_{ii}$$

with

$$\mathrm{disc}\,T_{ii} = T_{ii}(s+i\epsilon,t) - T_{ii}(s-i\epsilon,t).$$

Discontinuity, example: exp and its inverse log

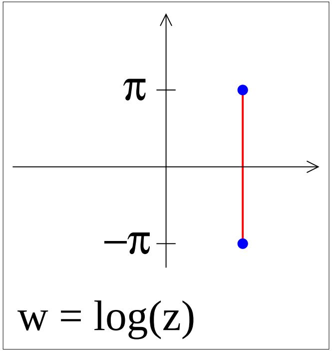

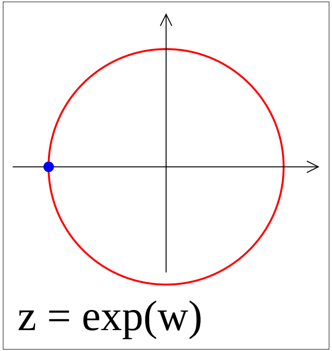

Problem: exp(w) maps two points to one,
inversion not possible

unless one excludes the green line

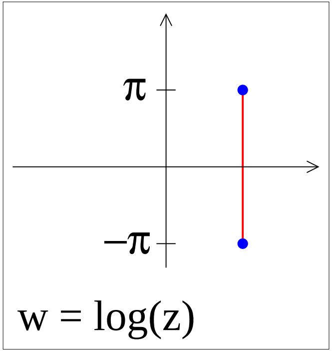

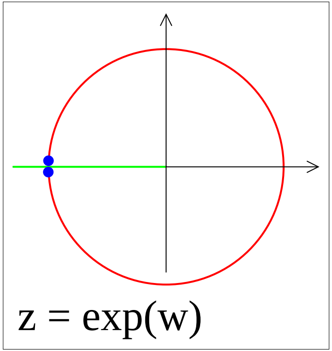

and shifts points on this line up or down (by ϵ).
Discontinuity = $2\pi i$

In detail: Let us study the mapping

$$w \to z \text{ with } z = \exp(w).$$

Consider $w = x + iy$, with x fixed and y going from $-\pi$ to π, which means we have a trajectory going from $w_1 = x - i\pi$ to $w_2 = x + i\pi$.
Doing the mapping $w \to z$ for this trajectory, we get

$$z = e^x e^{iy}$$

describing a circular trajectory with radius e^x with start and end point $z_1 = z_2 = -e^x$

Doing the inverse mapping $z \to w = \log(z)$: We get for $z_1 = z_2$ two different values w_1 and w_2 !!

One has to define log in $\mathbb{C} - \mathbb{R}_{\leq 0}$ (branch). The negative real axis is called branch cut.
The discontinuity at $z = -e^x$:

$$\log(z + i\epsilon) - \log(z - i\epsilon) = 2\pi i$$

Back to our T-matrix : We have

$$2s\,\sigma_{\mathrm{tot}} = \sum_f (2\pi)^4 \delta(p_f - p_i)\,|T_{fi}|^2 = \frac{1}{\mathrm{i}}\mathrm{disc}\,T_{ii}$$

$\frac{1}{\mathrm{i}}\mathrm{disc}\,\boldsymbol{T}$ can be seen as a so-called “cut diagram”, with modified Feynman rules, the “intermediate particles” are on mass shell, and we use simply

$$2s\,\sigma_{\mathrm{tot}} = \frac{1}{\mathrm{i}}\mathrm{disc}\,T_{ii}$$

Modified Feynman rules :

- □ Draw a dashed line from top to bottom

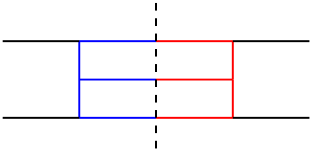

- □ Use "normal" Feynman rules to the left
- □ Use the complex conjugate expressions to the right
- □ For lines crossing the cut: Replace propagators by mass shell conditions $2\pi\theta(p^0)\delta(p^2 - m^2)$

Useful in case of substructures:

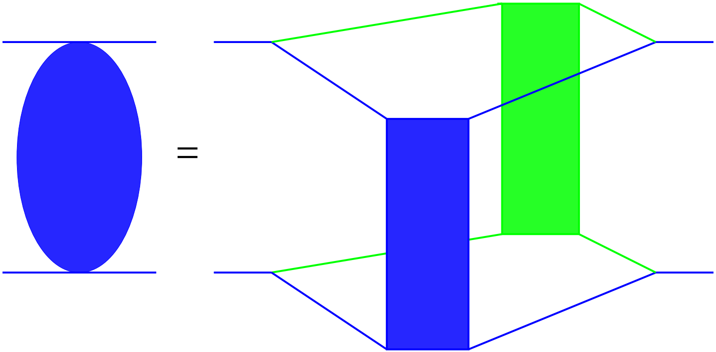

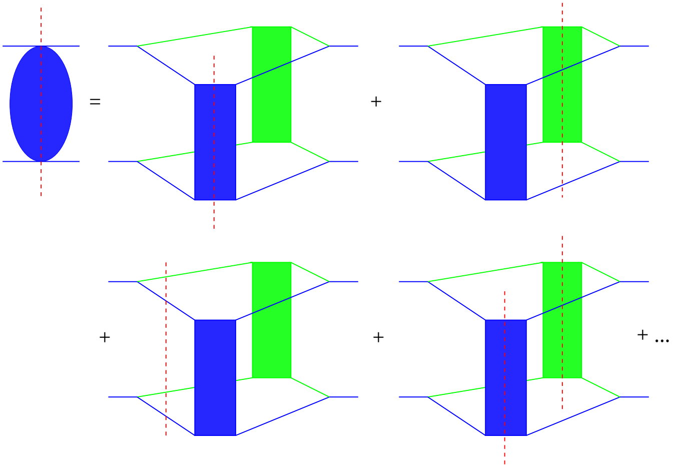

Cut diagram
= sum of products of cut/uncut subdiagrams

cut subdiagram

explicitely

symbol

mathematical expression

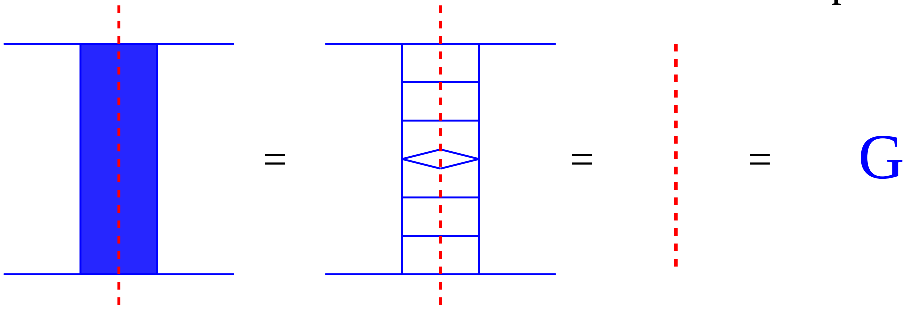

uncut subdiagram | explicitely | symbol | mathematical expression

=

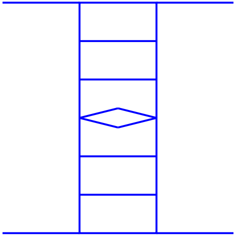

=

=

$-G$

Single Pomeron contribution G, computed via pQCD, can be (very well) fitted as*)

$$G \approx G_{\mathrm{fit}} = \alpha\,(x^{+})^{\beta}(x^{-})^{\beta'}$$

($x^{\pm}$are light cone momentum fractions)

Extremely useful! Allows analytical calculations of cross sections.

*) (Drescher, Hladik, Ostapchenko, Pierog, and Werner, Phys. Rept. 350, 2001)

Consistency requires adding more diagrams (ladder splitting/fusion, triple Pomeron vertices, gluon fusion in CGC ...)

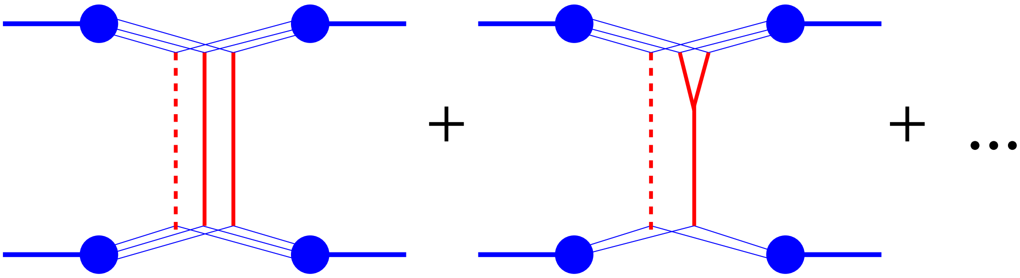

(Drescher, Hladik, Ostapchenko, Pierog, and Werner, Phys. Rept. 350, 2001)

Motivated by model calculations, we treat ladder fusion via adding an exponent [1] :

$$\boldsymbol{G_{\mathrm{fit}} \longrightarrow G_{\mathrm{eff}} = \alpha\,(x^{+})^{\beta+\varepsilon^{\mathrm{proj}}}(x^{-})^{\beta'+\varepsilon^{\mathrm{targ}}}}$$

("epsilon method") with

$$\varepsilon = \varepsilon(Z),$$

depending on "the number of participants":

$$Z^{\mathrm{proj}} = \sum_{\mathrm{proj\,nucleons\,i'}} f_{\mathrm{part}}\left(|\vec{b} + \vec{b_{i'}} - \vec{b_j}|\right)$$

(j is the target nucleon the Pomeron is connected to)

[1] K.Werner, FM.Liu, T.Pierog, Phys.Rev. C74 (2006) 044902

Advantages

- Cross section calculations perfectly doable
- Energy dependence of σ_{tot}, σ_{el} (and more) correct

Big problems

- **Adding ε does not change the internal Pomeron structure**
- No binary scaling in pA at high p_t (tails much too low)

Solution

- Introducing a **saturation scale**
  (K. Werner, B. Guiot, Iu. Karpenko, T. Pierog,
  Phys.Rev. C89 (2014) 064903)

Before: Compute G with fixed soft cutoff Q_0
$\longrightarrow$ fit $\longrightarrow$ add ε exponents

New: Compute G with saturation scale $Q_s \propto Z\,\hat{s}^{\lambda}$
$\longrightarrow$ fit (${\hat{s}}$ = Pomeron invariant mass)

varying Q_s changes internal structure!

Still something missing ...

- □ The saturation scale depends on the number of **participating nucleons**,

- □ but NOT on the **number of Pomerons** N_{Pom} (participating parton pairs)

The number of Pomerons represents the event activity in pp, as the number of participating nucleons does in pA.

The final solution

- □ Combining "epsilon method" and saturation scale in a smart way (T. Pierog and K. Werner, procs. EDS 2015, Borgo, France)

Step 1 Compute $G = G(Q_0)$ with fixed soft cutoff Q_0 $\rightarrow$ fit $\rightarrow$ add ε exponents ($\rightarrow$ G_{eff}) in order to fit cross sections

Step 2 Introduce saturation scale via

$$G_{\mathrm{eff}} = k\, G(Q_s)$$

affecting the internal structure

(We will see what to take to k)

The saturation scale Q_s^2

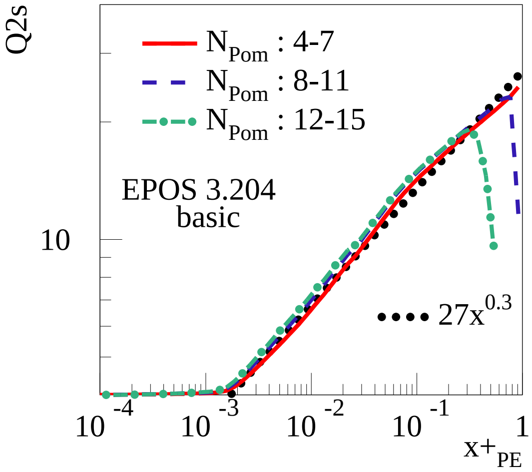

pp at 7 TeV

using $G_{\rm eff} = k\,G(Q_s)$

with constant k

($x+_{\rm PE}$ is the LC momentum fraction on the projectile side)

A crucial test:
Multiplicity dependence of spectra at high p_t

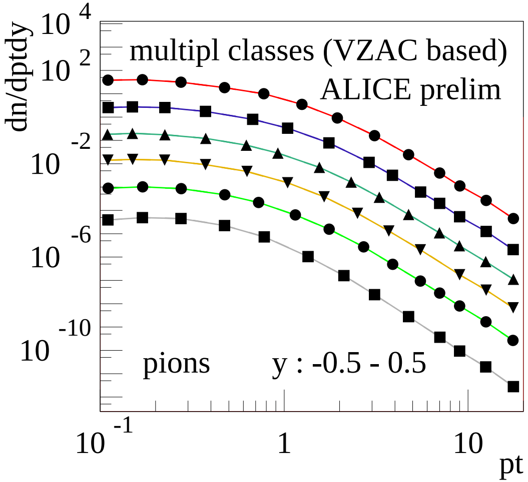

preliminary
ALICE data

(digitalized from B.A.Hess, talk at MPI@LHC 2015 Trieste November 27, 2015)

multiplicity bins (top to bottom):
0-1%, 1-5%, 10-15%, 20-30%, 40-50%, 70-100%

lines to guide the eye

Same data - ratio to 70-100%

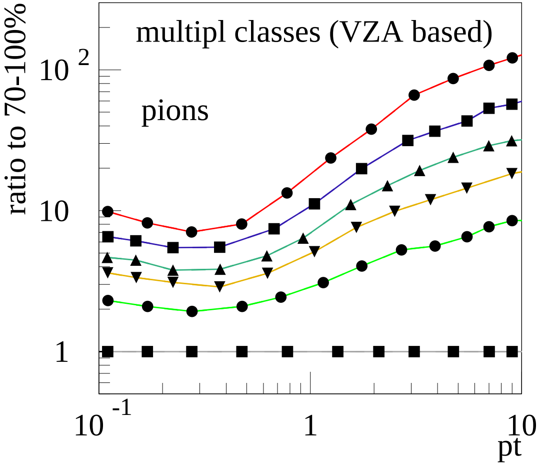

non-trivial:

spectra get harder with multiplicity

Comparing ALICE data with EPOS calculations

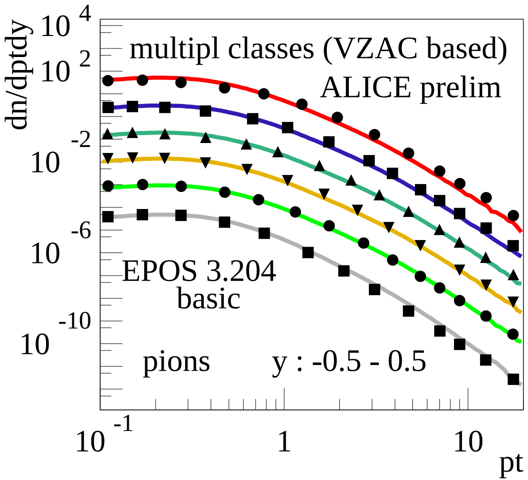

(preliminary ALICE data digitalized from B.A.Hess, talk at MPI@LHC 2015 Trieste November 27, 2015)

multiplicity bins
(top to bottom):
0-1%, 1-5%, 10-15%, 20-30%, 40-50%, 70-100%

Not too bad for a first shot ... but tails are not correct

Comparing ALICE data with EPOS calculations

Ratio calculation / data

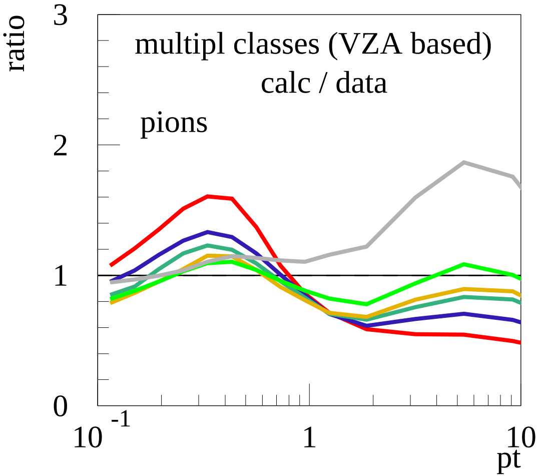

multiplicity bins :
0-1% (red) , 1-5%, 10-15%, 20-30%, 40-50%, 70-100% (grey)

Tails wrong by factors of two (low pt will be modified by hydro)

Make saturation scale Q_s^2 depending on N_{Pom}

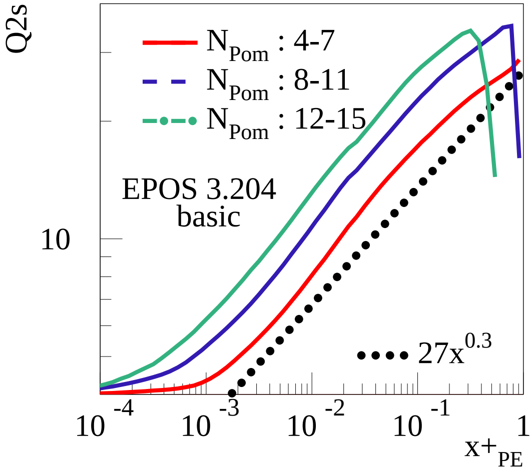

pp at 7 TeV

using $G_{\mathrm{eff}} = k\, G(Q_s)$

with

$$k = \left(\frac{N_{\mathrm{Pom}}}{\langle N_{\mathrm{Pom}} \rangle} \right)^{0.75}$$

higher Q_s^2 with increasing Pomeron number (like N_{part} dependence in pA)

Comparing ALICE data with EPOS calculations

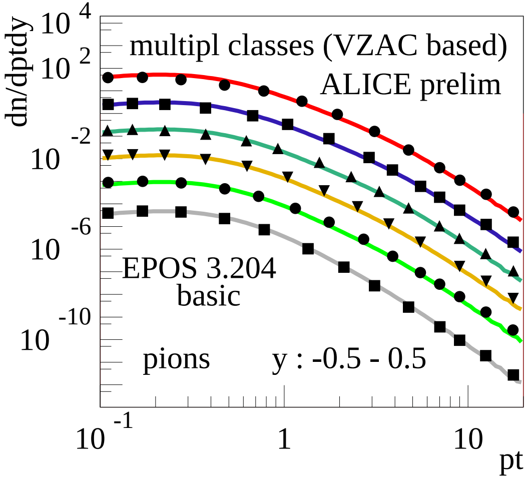

using

$$k = \left(\frac{N_{\mathrm{Pom}}}{\langle N_{\mathrm{Pom}}\rangle}\right)^{0.75}$$

=> much better

Comparing ALICE data with EPOS calculations
Ratio calculation / data

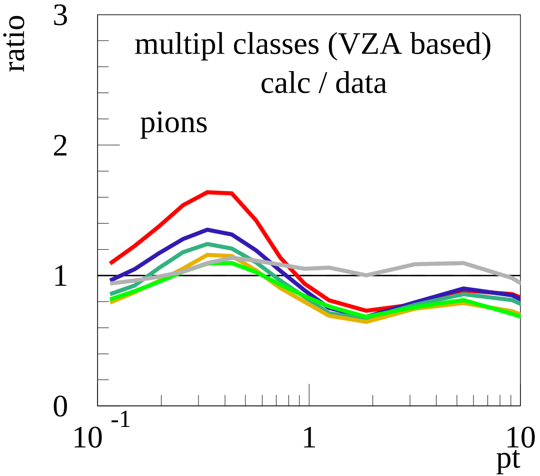

using

$$\boldsymbol{k} = \left(\frac{N_{\mathrm{Pom}}}{\langle N_{\mathrm{Pom}}\rangle}\right)^{0.75}$$

multiplicity bins : 0-1% (red) , 1-5%, 10-15%, 20-30%, 40-50%, 70-100% (grey)

Tails reasonable (low pt will be modified by hydro**)**

Still finetuning and tests needed, but we use

$$G_{\mathrm{eff}} = k\, G(Q_s)$$

with

$$k = \left(\frac{N_{\mathrm{Pom}}}{\langle N_{\mathrm{Pom}}\rangle}\right)^{A_{\mathrm{sat}}}, \quad A_{\mathrm{sat}} = 0.75$$

to analyse the multiplicity dependence of D-meson production (results depend somewhat on A_{sat})

Remark : This new procedure => EPOS 3.2xx

Part III

Multiplicity dependence of charm production

Notations (always at midrapidity) (D-meson = average D^+, D^0, D^{*+})

N_{ch} : **Charged particle multiplicity**

N_{D1} : **D-meson multiplicity for** $1 < p_t < 2\,\mathrm{GeV/c}$

N_{D2} : **D-meson multiplicity for** $2 < p_t < 4\,\mathrm{GeV/c}$

N_{D4} : **D-meson multiplicity for** $4 < p_t < 8\,\mathrm{GeV/c}$

N_{D8} : **D-meson multiplicity for** $8 < p_t < 12\,\mathrm{GeV/c}$

In addition we define normalized multiplitities

$$n = N/\langle N\rangle$$

for n_{ch} **and** n_{Di}

Heavy quark (Q) production in EPOS multiple scattering framework

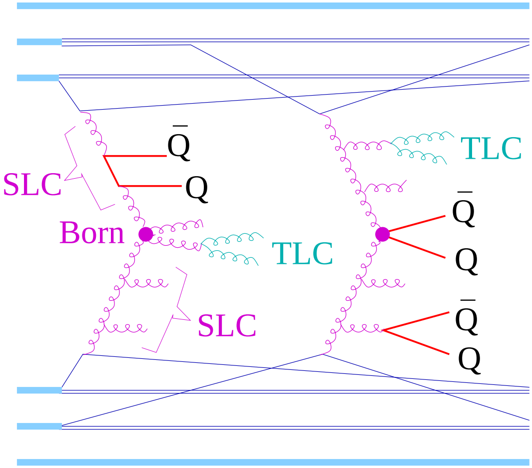

as light quark production

(but non-zero masses : $m_c = 1.3$, $m_b = 4.2$)

In any of the ladders

- ☐ **during SLC** (space-like cascade)
- ☐ **during TLC** (time-like cascade)
- ☐ **in Born**

Multiple scattering (EPOS3, basic):

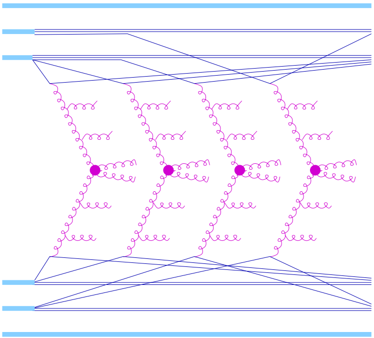

$$N_{Di} \propto N_{\mathrm{ch}} \propto N_{\mathrm{Pom}}$$

"Natural" linear behavior

(first approximation)

The actual calculations

n_{Di} vs n_{ch}

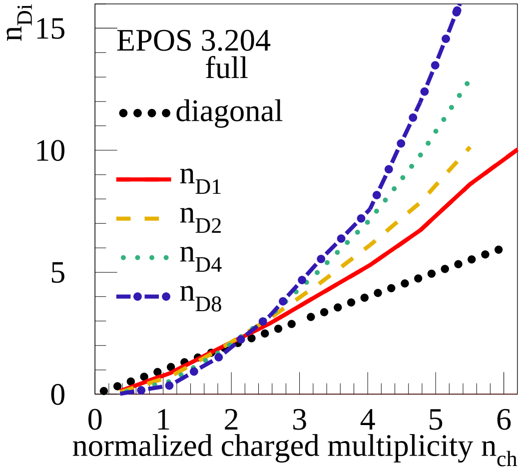

... even more than linear increase!

(in particular for large p_t)

(less for $A_{\mathrm{sat}} = 0$)

(much less in EPOS 3.1xx)

Why this pt dependence ?

Crucial: Fluctuations

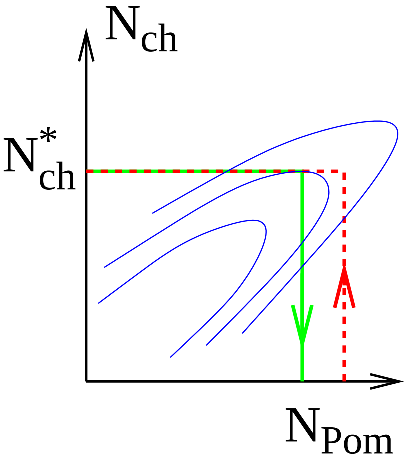

N_{ch} and N_{Pom}
are correlated,
but not one-to-one

(=> two-dimensional
probability distribution)

In the following, we consider fixed values $n_{\mathrm{ch}}{}^{*}$ of normalized charged multiplicities

To understand the implications of “fixed n_{ch}”

Strings in multiple scattering event (Schematic view):

basic EPOS

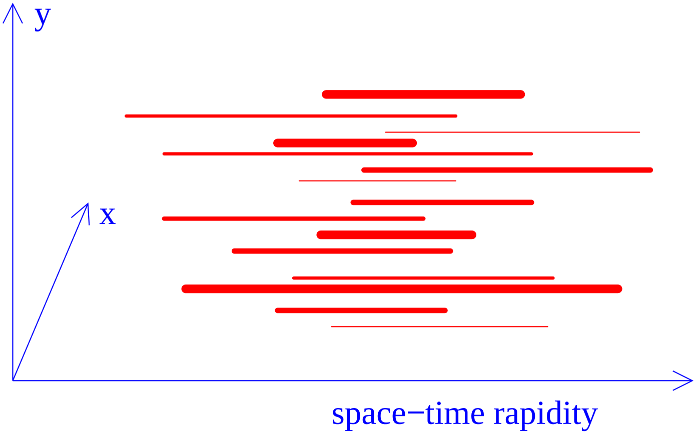

Strings of different lengths, different rapidity coverage, different hardness

length ~ mass ($\sqrt{x^+x^-s}$)

full EPOS (with hydro) string segments => fluid

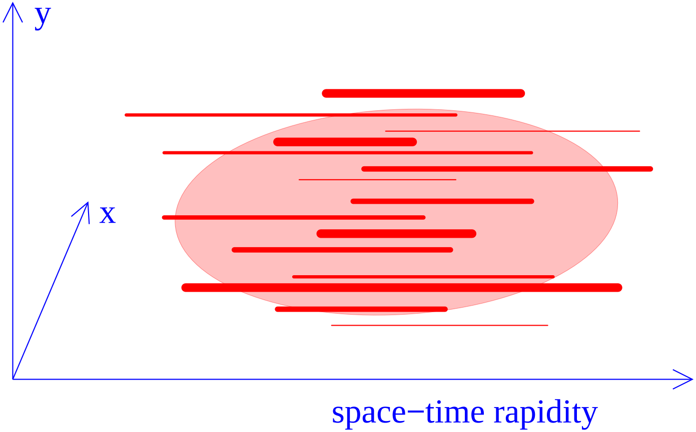

but
string properties
- number,
- masses,
- hardnesses

determine initial energy density and final multiplicity

Consider n_{D1} for some given $n_{ch}{}^*$

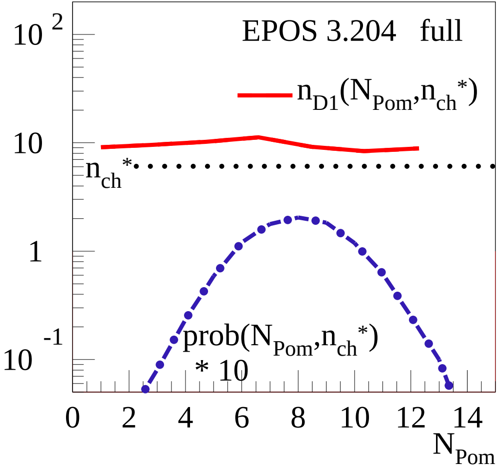

$$n_{D1} = \sum_{N_{\mathrm{Pom}}} \mathrm{prob}(N_{\mathrm{Pom}}, n_{\mathrm{ch}}{}^*) \times n_{D1}(N_{\mathrm{Pom}}, n_{\mathrm{ch}}{}^*)$$

$$\approx 1.6 \;\, n_{\mathrm{ch}}{}^*$$

having used

$$n_{D1}(N_{\mathrm{Pom}}, n_{\mathrm{ch}}{}^*) \approx 1.6\, n_{\mathrm{ch}}{}^*$$

The precise calculation (red point)

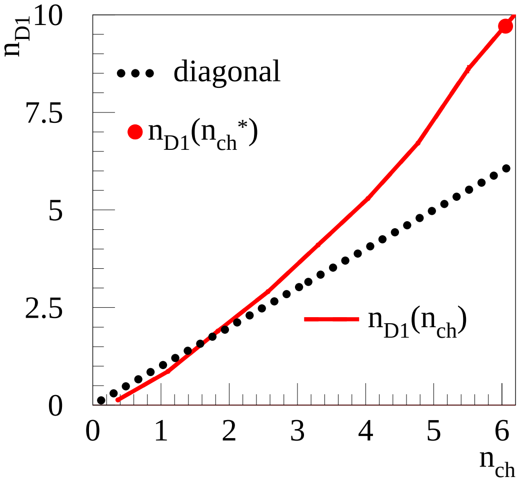

n_{D8} for given $n_{\mathrm{ch}}{}^{*}$

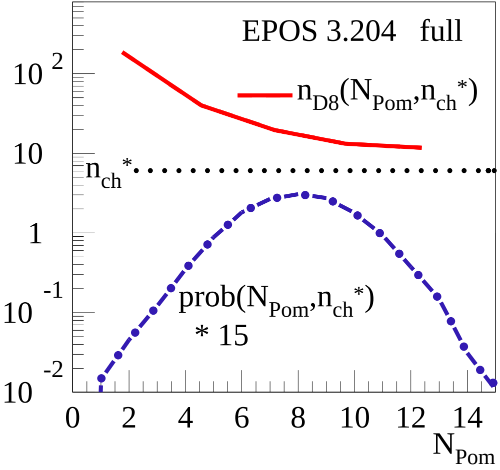

$$n_{D8} = \sum_{N_{\mathrm{Pom}}} \mathrm{prob}(N_{\mathrm{Pom}}, n_{\mathrm{ch}}{}^{*}) \times n_{D8}(N_{\mathrm{Pom}}, n_{\mathrm{ch}}{}^{*}) >> n_{\mathrm{ch}}{}^{*}$$

because
n_{D8} **>** $n_{\mathrm{ch}}{}^{*}$ **at high** N_{Pom}

and

increases strongly towards small N_{Pom}

The precise calculation (red point)

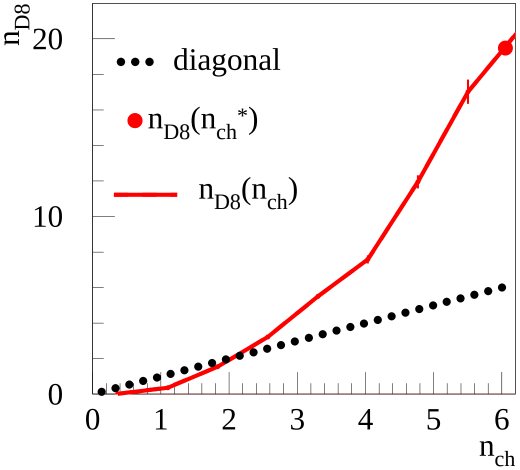

significantly above the diagonal!

strongly non-linear!

How to understand n_{D8} >> $n_{ch}{}^{*}$ and why increasing towards small N_{Pom}?

We compute in addition

- □ **The average invariant Pomeron mass for given N_{Pom} and $n_{\mathrm{ch}}{}^*$** (/ 100 GeV)

- □ **The average Pomeron hardness**

$$\left(\left\langle p_t^2\right\rangle / \left\langle p_t^2\right\rangle_{\mathrm{ref}} - 1\right) \times 100$$

for given N_{Pom} and $n_{\mathrm{ch}}{}^*$
(based on string segments; $\left\langle p_t^2\right\rangle_{\mathrm{ref}} = 0.55\,\mathrm{GeV}^2$)

Pomeron mass and hardness

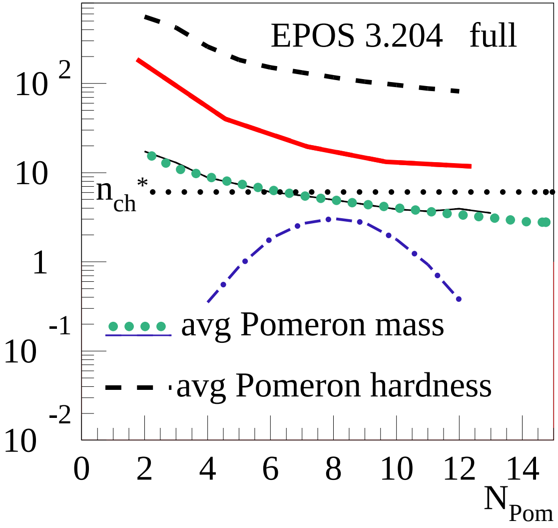

both increase significantly with decreasing N_{Pom}

red line: n_{D8}

blue dashed-dotted: N_{Pom} distr

correspondence hardness - n_{D8} !!

Strong non-linear increase (of $n_{D8}(n_{\mathrm{ch}})$) since

- Pomerons harder with increasing multiplicity (more screening, higher Q_2^s)

- The number of Pomerons fluctuates for given multiplicity and smaller Pomeron numbers imply harder Pomerons

- note : n_{D8} is nothing but a “Pomeron hardness” measure (even a very sensitive one)

EPOS 3.204 compared to data

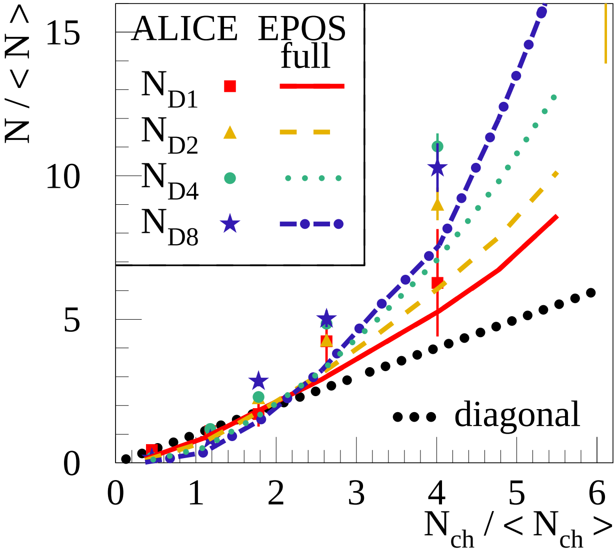

Hydo helps somewhat

(for basic EPOS the increase is somewhat less)

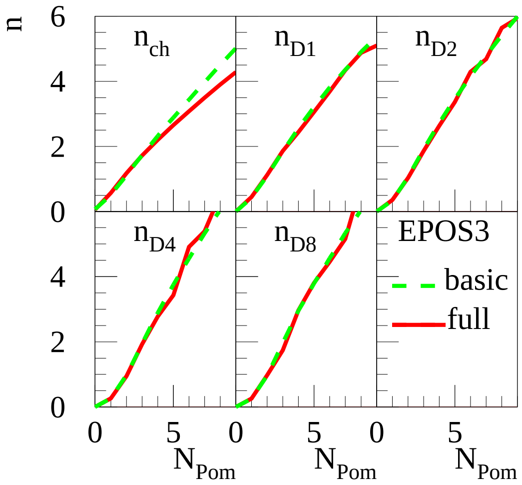

No change for n_{Di}

But some reduction of n_{ch}

=> $n_{D8}(n_{ch})$ with hydro is somewhat steeper compared to basic EPOS

Why multiplicity reduction?

Basic EPOS:
Pomerons > Strings
> String fragmentation
(independent of event activity)

Full model:
Pomerons > Strings
> Fluid, collectivity
(collective energy increases with event activity)

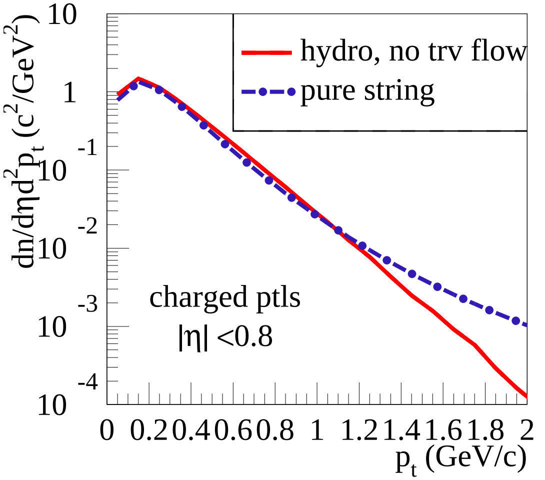

Taking charged-particle multiplicity at forward/backward rapidity

$$2.8 < \eta < 5.1 \quad \text{and} \quad -3.7 < \eta < -1.7$$

(Vzero multiplicity, N_{vz}**,** n_{vz}**)**

Vzero multiplicity : Smaller increase

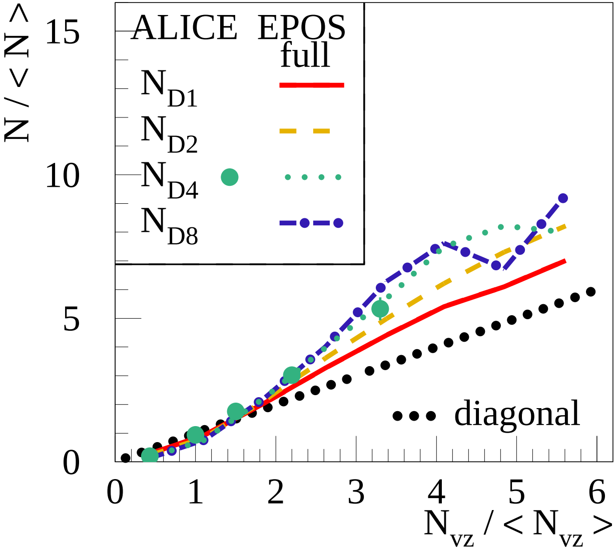

as in the data

n_{D8} for given $n_{\mathrm{vz}}{}^{*}$

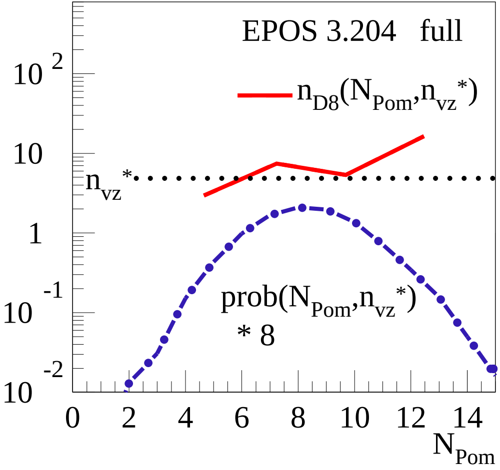

whereas

$n_{D8}(N_{\mathrm{Pom}}, n_{\mathrm{ch}}{}^{*})$
increases strongly towards small N_{Pom}

$n_{D8}(N_{\mathrm{Pom}}, n_{\mathrm{vz}}{}^{*})$
decreases slightly

=> Pomerons do not get harder

Why do Pomerons get harder at small N_{Pom} for fixed n_{ch} but not for fixed n_{vz} ?

In case of n_{ch}, almost all Pomerons cover the corresponding central rapidity range

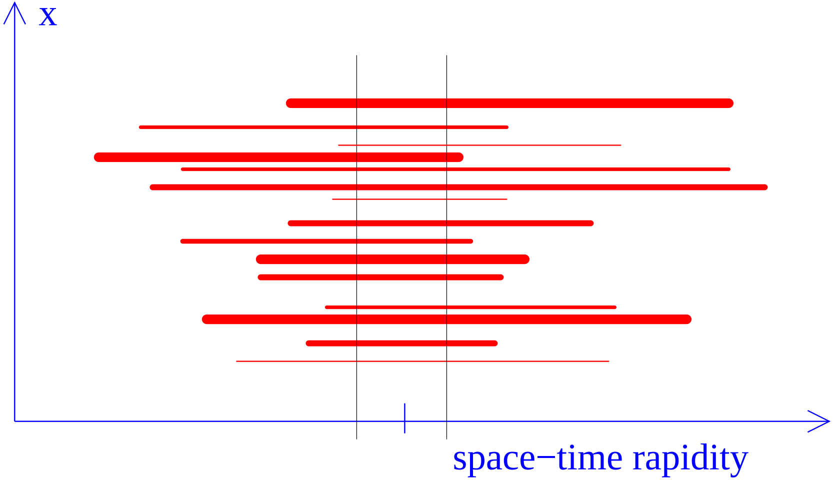

In case of n_{ch}, almost all Pomerons cover the corresponding central rapidity range, so to keep n_{ch} fixed for smaller N_{Pom} requires harder Pomerons (no other way)

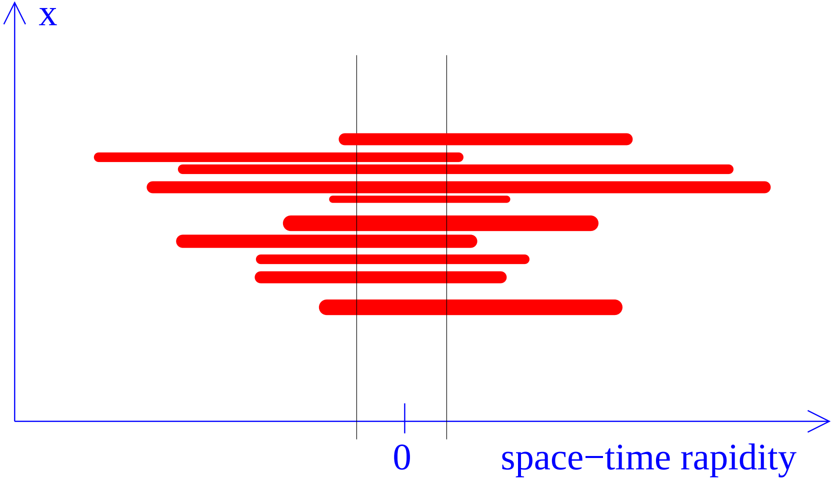

Side remark:

In principle a possibility to define

- **particular event classes, with essentially "hard" Pomerons,**

- **by triggering on high multiplicity AND large D meson yields**

In case of n_{vz}, only some Pomerons cover the corresponding forward rapidity range,

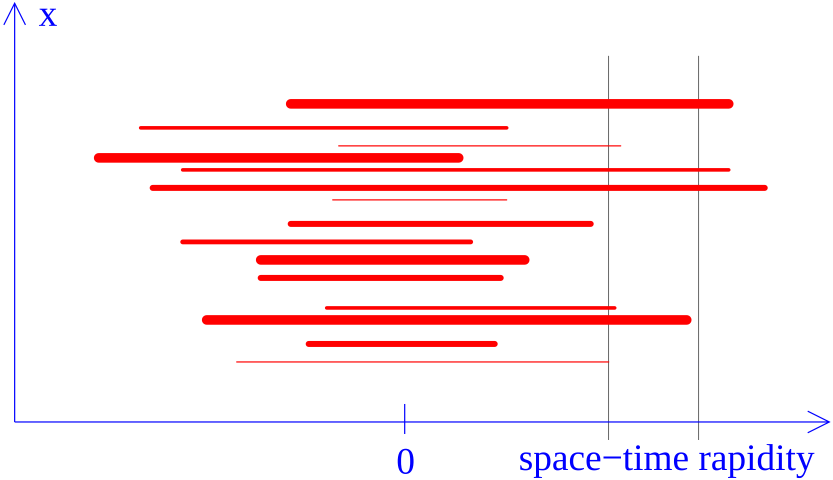

In case of n_{vz}, only some Pomerons cover the corresponding forward rapidity range, so to keep n_{vz} fixed for smaller N_{Pom} can be accomodated with more Pomerons covering that rapidity range

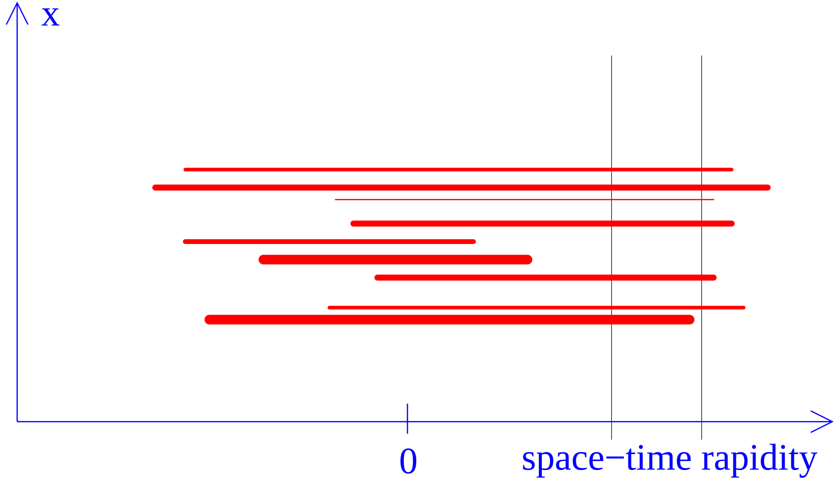

Summary

- **New (and final?) major improvement of the multiple scattering scheme in EPOS: Pomeron number dependence of the saturation scale** (**and the corresponding technical improvements which make it possible**)
- **Provides increasing Pomeron hardness with increasing multiplicity** (**ALICE multipl dependence of spectra**)
- **Explains strong increase of high pt charm production vs multiplicity, and the modest increase in case of forward multiplicity.**